Article

Self-Assembly of Hydrogen-Bonded Fibrous Fe^{II} Triazole Complexes and Their Spin Crossover Characteristics in Organic Media

Keita Kuroiwa *,†, Yukari Jo, and Nobuo Kimizuka

Department of Chemistry and Biochemistry, Graduate School of Engineering, Kyushu University, 744 Moto-oka, Nishi-ku, Fukuoka 819-0395, Japan

* Correspondence: keitak@nano.sojo-u.ac.jp

† Current address: Department of Nanoscience, Faculty of Engineering, Sojo University, 4-22-1 Ikeda, Nishi-ku, Kumamoto 860-0082, Japan.

Received: 20 February 2025; Revised: 30 May 2025; Accepted: 3 June 2025; Published: 6 June 2025

Abstract: The lipophilic linear Fe^{II} triazole complexes $[Fe^{II}(\mathbf{L})_3]Cl_2$ (**L** = **1**–**5**) were synthesized using ligands **1**–**5** containing amide bonds between alkyl chains and 1,2,4-triazole ligands with various spacer methylene length. When the amido and ether linkages are introduced in the alkyl chain moiety, the iron complexes are dissolved in chloroform, $[Fe^{II}(\mathbf{1})_3]Cl_2$ forms a pale purple jelly-like phase. The purple color is accompanied by a structured absorption around 540 nm, characteristic of iron (II) in the low spin (LS) state. Atomic force microscopy (AFM) and transmission electron microscopy (TEM) of the jelly-like phase confirm the formation of networks of fibrous nano assemblies with widths of 10–30 nm. The observed widths are larger than the molecular lengths of the triazole ligands. The pale purple jelly-like phase turned into a pale-yellow solution by heating above ca 310 K, indicating the formation of high spin (HS) state complexes. The complexes show irreversible spin crossover in the solid state, characterized by SQUID. Interestingly, an abrupt spin crossover is observed in solution reversibly with some thermal hysteresis. UV-vis spectra also showed reversible spin crossover phenomena dependent on the spacer length between the amide group and the Fe(II) triazole complexes. IR spectra of these complexes in chloroform show the formation of hydrogen bonding from amide groups, which enhanced alkyl-chain packing in the coordination polymers. The freeze-dried iron triazole complexes form lamellar structures, which indicates the alkyl chains extending radially from the octahedral triazole complex moiety are oriented in a lamellar packing due to the presence of flexible ether linkages in alkyl chains, which allowed decoupling the alignment of the dodecyloxy alkyl chains from the spacer methylenes connected to the Fe(II) triazole complexes. Introducing amide bondages to the lipophilic one-dimensional coordination systems stabilizes the low-spin state by hydrogen bond networks. It provides hysteresis in the spin crossover in solution, ascribed to the recombination of hydrogen bonds during the temperature change between the heating and cooling sides. Combining hydrogen bonds and lipophilic one-dimensional complexes provides a valuable means to enhance their stability and control physical properties in solution.

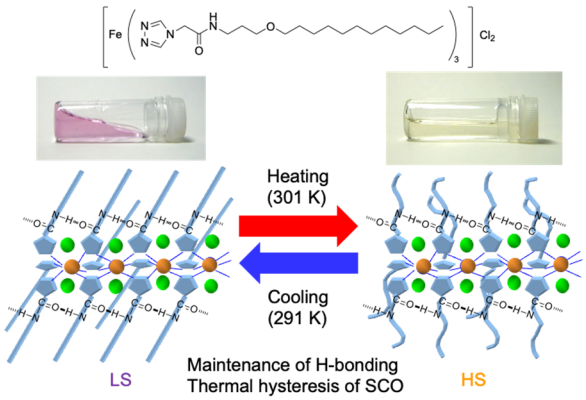

Keywords: spin crossover; thermal hysteresis; nano metal complex; coordination polymer; self-assembly

1. Introduction

The concept of spin crossover (SCO) was first introduced by Cambi and colleagues in the 1930s [1]. Since then, a significant number of SCO compounds have been reported, particularly those in solid-state materials. The phenomenon of spin crossover with hysteresis, realized by strong cooperative effects, has attracted much attention due to its potential applications in magnetic devices and information storage materials [2,3]. Cooperativity, a crucial phenomenon, facilitates the propagation of spin state information from a metal complex to neighboring

complexes, resulting in collective spin state transitions throughout the system. In crystalline solids, the degree of cooperativity is determined by the interactions between neighboring metal complexes, which are influenced by the molecular structure of metal complexes, intermolecular interactions, and molecular arrangement in crystals. Achieving enhanced cooperativity in spin-crossover systems with long-range interactions between metal ion units is essential. Realizing such cooperativity in one-dimensional (1D), two-dimensional (2D), or three-dimensional (3D) networks, along with the rational control of the spin crossover behavior is essential to develop next-generation materials with quantum spin functions [4–12].

In particular, the spin crossover properties of 1D iron(II) triazole complexes have been studied extensively by both chemists and physicists. For instance, Kahn and his collaborators reported that mixed-ligand iron(II) triazole complexes exhibit abrupt spin crossover with sizeable thermal hysteresis near room temperature [3,13]. After this seminal work, iron(II) triazole complexes were recognized as promising candidates for magnetic devices. These complexes have been studied in bulk crystalline forms and other matrices, including polymer films [14–16], polymer derivatives [17–20], and surfactant-capped crystalline nanoparticles [21,22]. Thus, iron(II) triazole complexes serve as spin crossover materials that can be realized in bulk solids and various material systems [23–25].

In addition to the conventional studies focusing on the solid state, spin crossover has also been investigated for monomeric complexes in solutions, [26–32] self-assembly in liquid crystals or gels [25,33–38], and polymer-hybrid systems in gels [39–42]. In solutions, molecularly dissolved iron(II) complexes show spin equilibrium without hysteresis. Metal complexes in gels are more or less solvated by solvent molecules, resulting in a substantial reduction in the cooperativity that requires strong intermolecular interactions. The spin crossover observed for these solutions and gels generally reflects the thermal equilibrium of each complex governed by the Boltzmann distribution, resulting in gradual changes [27–32]. It is widely observed that metal complexes exhibiting abrupt spin crossover in the solid state exhibit a smooth spin equilibrium in solution [43–45], and it remains a challenge to develop molecular design principles to achieve cooperative spin crossover with hysteresis in organic media.

To address this issue, we have developed lipophilic bridging triazole ligands by introducing an alkyl chain containing a flexible ether linkage to disperse one-dimensional triazole complexes as nanowires in organic media [46–53]. Iron(II) complexes bearing 4-dodecyloxypropyl-1,2,4-triazole ligands revealed a low-spin (LS) state in solid or film state and formed organogels when dispersed in organic solvents such as chloroform. Meanwhile, the low-spin (LS) state is destabilized in gels due to the solvation of alkyl chains that increased the Fe-Fe distances, and the gels showed a high-spin (HS) state. To overcome the destabilization of the LS state based on the solvation of the lipid-soluble alkyl chains directly bound to the triazole ligand, we introduced anionic lipids as counter anions of the 1D iron(II) 1,2,4-triazole complexes [54]. This supramolecular approach led to a remarkable stabilization of LS complexes in organic media. It enabled spin conversion, i.e., the spin control via temperature-dependent dynamic self-assembly of linear coordination chains [54]. These results indicate the importance of supramolecular stabilization of LS complexes and self-assembly as valuable strategies for improving spin crossover phenomena in soluble coordination polymer systems.

In this study, we introduced hydrogen bond networks to stabilize the LS state of 1D iron(II) 1,2,4-triazole complexes. We developed new ether-lipophilic triazole ligands containing an amide bondage. These complexes were dispersible in organic media, and we investigated their spin crossover properties in solutions and gels. We found that hydrogen bonding enhances the thermal stability of the low-spin (LS) state in solution. In addition, after the LS-HS transition by heating, the reversed HS-LS transition during the cooling process showed thermal hysteresis originating from the recombination process of hydrogen bonds. The cooperative spin crossover behavior is discussed regarding the structural changes of iron(II) 1,2,4-triazole complexes and their mesoscopic nanostructures formed by self-assembly. These findings provide a simple and valuable means to regulate the self-assembly behavior of iron(II) 1,2,4-triazole complexes and their spin crossover characteristics.

2. Experimental Section

2.1 Materials

Reagents and solvents were obtained from commercial sources. Anhydrous chloroform and methanol were obtained by distillation over $CaCl_2$ and CaH_2, respectively. The product was synthesized according to the previous report (see Supporting Information) [55]. The structures of triazole derivatives and the final ligands were confirmed by thin-layer chromatography, Fourier Transform Infrared Spectroscopy (FT-IR PreStage21, Shimadzu, Kyoto, Japan) and Nuclear Magnetic Resonance (NMR) spectroscopies (DRX600, 600 MHz, Bruker, Billerica, MA, USA), and elemental analysis.

2.2 Measurements

Ultraviolet-visible (UV-vis) spectra were measured on V-550, V-560, or V-570 spectrophotometer (JASCO, Tokyo, Japan). Transmission electron microscopy (TEM) was conducted on a JEM-2010 (JEOL, Tokyo, Japan), operating at 120 kV. Specimens for TEM were prepared by transferring the surface layer of gels or solutions on carbon-coated TEM grids or HOPG [56]. Atomic force microscopy (AFM, contact mode) was carried out with a PicoPlus microscopy (Molecular Imaging, Tempe, AZ, USA) with a cantilever of SI-AF01. Specimens for AFM observations were prepared by using a freshly cleaved, highly oriented pyrolytic graphite (HOPG, ZYA, 10 × 10 mm^2, NT-MDT Co., Tempe, AZ, USA). Differential scanning calorimetry (DSC) was conducted on an SSC-5200H instrument (Seiko Instruments Inc., Chiba, Japan) (heating rate = 1 K min^{-1}). Samples for DSC measurements were placed in an aluminum pan (SSC000E33, Seiko Instruments Inc., Chiba, Japan). Magnetic susceptibility measurements were performed on an MPMS-7XL superconducting quantum interference device (SQUID) magnetometer (Quantum Design, San Diego, CA, USA) in a temperature range of 100–400 K (solid state) and 210–350 K (liquid state). Magnetic data were corrected for diamagnetic contributions from triazole ligands and sample holders. The Pascal constants of the ligands and susceptibilities of the holders, which were measured separately, were used for the correction. The wide-angle X-ray diffraction (WAXD) data were recorded on a powder X-ray diffractometer at BL02B2 in SPring-8 (Hyogo, Japan; operation energy = 8 GeV, stored current = 100 mA, λ = 1 Å). For XRD, samples are placed in a capillary (Markrohrchen aus Glas Nr. 14, 80 mm(long) × 0.5 mm(diameter) × 0.01 mm(thick)), Hilgenberg GmbH, Malsfeld, Germany).

3. Result and Discussion

The lipophilic triazole ligands **1**–**5** (Scheme 1) were synthesized by modifying the literature method [55]. A flexible ether linkage was introduced in **1**–**5**, since it enhances the solubility in organic media and provides the packing of alkyl chains in the supramolecular assemblies [57–61] and coordination polymers [46,48–52]. The iron triazole complexes containing ligands **1**–**5** were prepared by mixing each ligand with $FeCl_2$ in dry methanol at room temperature and were obtained as powders.

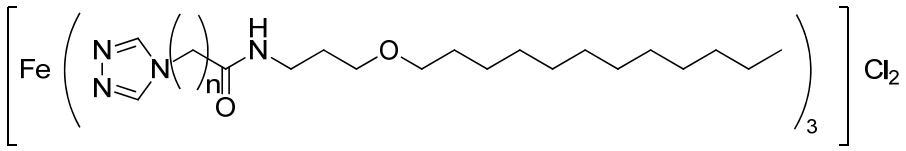

$[Fe(L)_3]Cl_2$

L = 1(n = 1), **2** (n = 2), **3** (n = 3), **4** (n = 4), and **5** (n = 5)

Scheme 1. Chemical structure of $[Fe(\mathbf{L})_3]Cl_2$, (**L** = **1**–**5**).

When $[Fe^{II}(\mathbf{1})_3]Cl_2$ was dissolved in chloroform, a pale purple jelly-like solution was formed at room temperature (concentration, 5 unit mM, Figure 1a). Here, the "unit mM" refers to the concentration per $[Fe(\mathbf{1})_3]^{2+}$ monomeric unit of the coordination polymer. Upon heating, the jelly-like solution turned to a yellow solution above the temperature of ca. 310 K (Figure 1b). It indicates that the LS state is thermally stabilized by possibly polymeric self-assemblies that form the jelly-like solution. In contrast, the complex in the HS state does not retain the jelly-like solution and is dispersed in chloroform. The pale purple jelly-like solution was also formed in the case of $[Fe^{II}(\mathbf{2})_3]Cl_2$. On the other hand, the complex with a more extended spacer methylene unit $[Fe^{II}(\mathbf{3})_3]Cl_2$ formed a colorless, i.e., HS-state jelly-like solution, indicating the absence of LS species. The longer-spacer compounds $[Fe^{II}(\mathbf{4})_3]Cl_2$ and $[Fe^{II}(\mathbf{5})_3]Cl_2$ were dispersed in chloroform without forming jelly-like solutions at 5 unit mM. These results indicate that the solution characteristics depend on the spacer length between the dodecyloxypropyl chain and the triazole ring, and their solution properties and spin state are controlled by the spacer moiety. The spacer-length-dependent properties of the solution are further examined in detail, as discussed later, by FT-IR spectroscopy and wide-angle X-ray diffraction.

Atomic force microscopy (AFM) was performed to investigate the morphology of the coordination structures. Figure 2a shows an AFM image of $[Fe^{II}(\mathbf{1})_3]Cl_2$ transferred on highly oriented pyrolytic graphite (HOPG). Networks of fibrous nanoassemblies with a width of 10–30 nm are abundantly observed. Transmission electron microscopy (TEM) was also conducted to investigate $[Fe^{II}(\mathbf{1})_3]Cl_2$ transferred onto a carbon-coated copper grid (Figure 2b). Fibrous nanostructures with a width of 20–50 nm are abundantly seen. The formation of the fibrous nanostructures are also observed for the other iron triazole complexes $[Fe^{II}(\mathbf{2}–\mathbf{5})_3]Cl_2$ ($[Fe^{II}(\mathbf{2})_3]Cl_2$, 10–30 nm, Figure S1a; $[Fe^{II}(\mathbf{3})_3]Cl_2$, 10–30 nm, Figure S1b; $[Fe^{II}(\mathbf{4})_3]Cl_2$, 10–50 nm, Figure S1c; $[Fe^{II}(\mathbf{5})_3]Cl_2$, 10–50 nm,

Figure S1d). Since the molecular length of ligands **1**–**5** is in the range of 26–32 Å (**1**, 26.5 Å; **2**, 27.1 Å; **3**, 29.0 Å; **4**, 30.0 Å; **5**, 31.5 Å, estimated by Corey–Pauling–Koltun (CPK) model), the widths of fibrous structures are larger than twice the molecular length of ligands. Therefore, they comprise a few strands of linear triazole complexes, as schematically shown in Figure 2c.

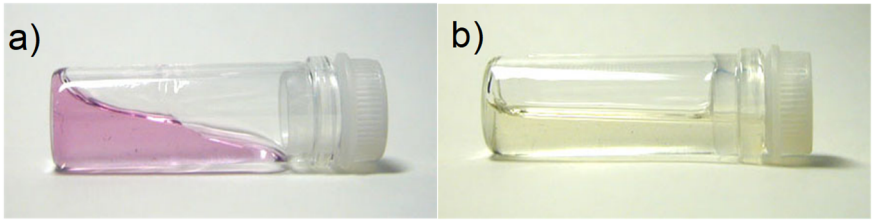

Figure 1. Pictures of $[Fe(\mathbf{1})_3]Cl_2$ in chloroform: (**a**) a pale purple jelly-like phase at 298 K. (**b**) a pale yellow solution at 323 K.

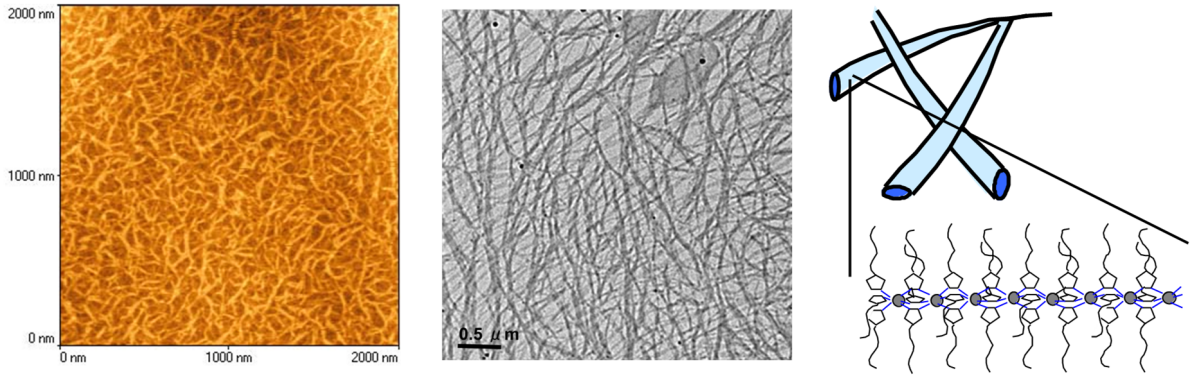

Figure 2. (**a**) AFM image of $[Fe(\mathbf{1})_3]Cl_2$ (5 unit mM) transferred on HOPG. (**b**) TEM image of $[Fe(\mathbf{1})_3]Cl_2$ (5 unit mM) transferred on a carbon-coated TEM grid. (**c**) Schematic illustration of iron triazole complexes in fibrous nanofiber.

Figure 3 compares the temperature dependences of the magnetic susceptibility for $[Fe^{II}(\mathbf{1})_3]Cl_2$ in chloroform and that observed for the powdery $[Fe^{II}(\mathbf{1})_3]Cl_2$. In the solid state, $[Fe^{II}(\mathbf{1})_3]Cl_2$ exhibits a spin crossover upon heating at 340 K, whereas the HS state was maintained during the cooling process to 200 K (Figure 3a). It indicates the spin crossover is irreversible in the solid state. On the other hand, $[Fe^{II}(\mathbf{1})_3]Cl_2$ in chloroform provides reversible spin crossover with thermal hysteresis around room temperature. Spin crossover temperature (T_{sc}) was 301 K ($T_{sc}\uparrow$) and 291 K($T_{sc}\downarrow$, Figure 3b). T_{sc} is the temperature at which the crossover produces a half-fraction of the HS state. Surprisingly, the spin crossover of $[Fe^{II}(\mathbf{1})_3]Cl_2$ in chloroform was accompanied by thermal hysteresis, although the coordination polymer was dispersed as fibrous nanostructures. To confirm the presence of thermal hysteresis, we measured the temperature dependence of UV-vis absorption spectra for $[Fe^{II}(\mathbf{1})_3]Cl_2$ dispersed in chloroform, as shown in Figure 4a. At lower temperatures, a peak is observed around 528 nm, ascribed to the $^1A_1 \rightarrow {}^1T_1$ transition of the LS complex. Upon heating the LS dispersion, the intensity of the $^1A_1 \rightarrow {}^1T_1$ transition decreased, while a new peak appeared around 800 nm. This near-infrared peak is assigned to a *d-d* transition of the HS complex ($^5T_2 \rightarrow {}^5E$). Upon cooling the HS dispersion to 265 K, a reversible spectral change was observed with thermal hysteresis, which is in good agreement with the result of magnetic susceptibility measurement ($[Fe^{II}(\mathbf{1})_3]Cl_2$, $T_{sc}\uparrow$ 301 K, $T_{sc}\downarrow$ 291 K, Figure 4b).

To date, thermal hysteresis of the spin crossover exerted by one-dimensional coordination polymers is observed in bulk or nano-crystalline structures, indicating that the expression of cooperativity requires crystalline order [6–12]. When Fe(II) 1,2,4-triazole complexes are dispersed in organic media as nanofibers, thermal hysteresis is not observed in their spin crossover [46,48,49,51]. Therefore, the thermal hysteresis observed for $[Fe^{II}(\mathbf{1})_3]Cl_2$ in chloroform indicates that the hydrogen bonding enhances the cohesive forces operating among ligand alkyl chains and effectively stabilize the LS complexes.

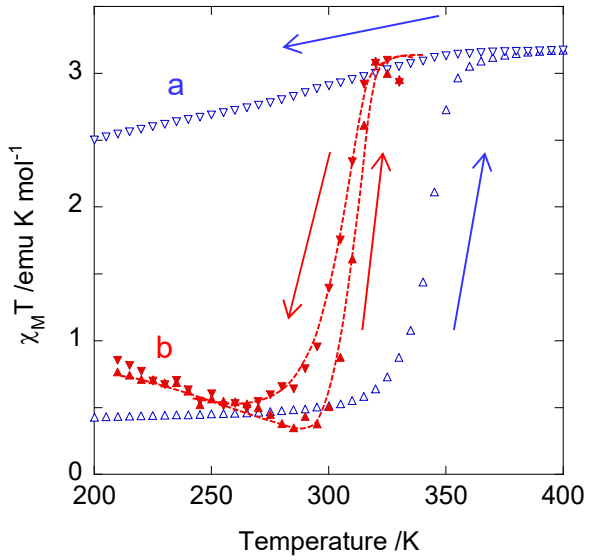

Figure 3. Temperature dependence of magnetic susceptibility $\chi_M T$ of $[Fe(\mathbf{1})_3]Cl_2$ in solid state (blue symbols and arrows) (**a**), and in chloroform (5 unit mM, red symbols and arrows) (**b**). The arrows accompanying the ▲(△) or ▼(▽) symbols represent the heating or cooling processes, respectively. These data suggest reversibly thermal hysteresis in solution, in contrast to irreversible changes observed in the solid state.

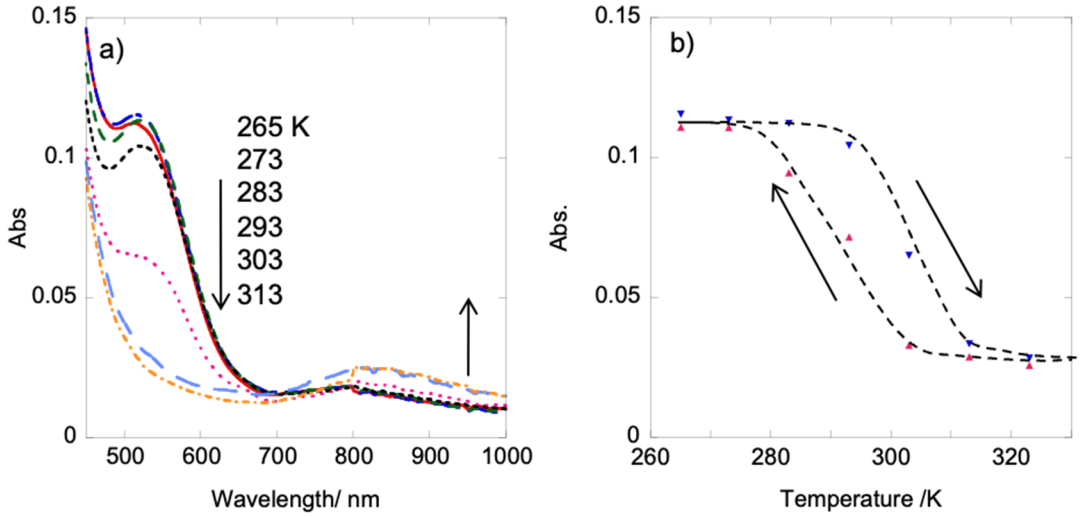

Figure 4. (**a**) Temperature dependence of UV-vis spectra of $[Fe(\mathbf{1})_3]Cl_2$ in chloroform (5 unit mM). The arrows indicate a decrease in the LS-derived absorption band at 528 nm and an increase in the HS-derived band around 800 nm upon heating from 265 K to 313 K. (**b**) Temperature dependence of the absorption intensity (at 540 nm) during the heating and cooling cycles. The arrows accompanying the ▼ or ▲ symbols represent the heating or cooling processes, respectively.

Figure S2 shows temperature dependences of the absorbance at 528 nm (LS species) during the heating and cooling cycles, observed for $[Fe^{II}(\mathbf{L})_3]Cl_2$ (**L** = **2**–**5**). All these complexes showed spin crossover phenomena with weak thermal hysteresis around ambient temperatures. The temperature ranges of spin crossover shifted to lower temperatures for complexes containing more extended spacer unit ($[Fe^{II}(\mathbf{2})_3]Cl_2$, T_{sc}↑ 293 K, T_{sc}↓ 292 K, Figure S2a; $[Fe^{II}(\mathbf{3})_3]Cl_2$, T_{sc}↑ 298 K, T_{sc}↓ 289 K, Figure S2b; $[Fe^{II}(\mathbf{4})_3]Cl_2$, T_{sc}↑ 292 K, T_{sc}↓ 281 K, Figure S2c; $[Fe^{II}(\mathbf{5})_3]Cl_2$, T_{sc}↑ 287 K, T_{sc}↓ 282 K, Figure S2d). Among these complexes, however, we note that the complex $[Fe^{II}(\mathbf{2})_3]Cl_2$ did not show sufficient thermal hysteresis despite those observed for the iron(II) triazole complexes with longer-spacer chains (L = **3**, **4**, and **5**, Figure S2a). The peculiar absence of a distinct thermal hysteresis in $[Fe^{II}(\mathbf{2})_3]Cl_2$, in contrast to the behavior observed for the longer-spacer analogues ($[Fe^{II}(\mathbf{L})_3]Cl_2$, **L** = **3**, **4**, and **5**), is further discussed in terms of molecular packing based on the wide-angle X-ray diffraction analysis (discussed later). Moreover, the observed stabilization of the low-spin (LS) state as the spacer length decreases can be attributed to the closer proximity between the hydrogen-bonding amide moieties and the triazole rings, as described by the FT-IR spectra in the following paragraph. In particular, in chloroform, effective intermolecular hydrogen

bonding between the amido linkages is more likely to occur due to this structural proximity, which can restrict the molecular mobility of the triazole complexes. This suppression of dynamic motion may result in enhanced spin compaction and a preference for the LS state even at relatively higher temperatures.

Fourier transition infrared (FT-IR) spectra of iron triazole complexes, $[Fe^{II}(\mathbf{L})_3]Cl_2$ (**L** = **1**–**5**) in chloroform were measured at varied temperatures to investigate the relevance of hydrogen bonding between amide bonds to the observed thermal hysteresis. Chloroform dispersions of $[Fe^{II}(\mathbf{L})_3]Cl_2$ (**L** = **1**–**5**) were introduced into a thin layer cell made of NaCl (Figure S3). In the course of heating chloroform dispersion of $[Fe^{II}(\mathbf{1})_3]Cl_2$, C=O stretching (ν(C=O)) and N-H vending (δ(N-H)) vibrations were observed at 1680 and 1561 cm^{-1}, respectively (Temperatures at 278 K and 293 K, Figure S3a). These peaks indicate the formation not only of intermolecular hydrogen bonding among amido groups, but also intermolecular hydrogen bonding between amido group and halide anion, and intramolecular hydrogen bonding between amido group and C-H of triazole ligand [62,63]. In addition, a C=N stretching vibration (ν(C=N)) of the triazole unit was seen at 1416 cm^{-1}, characteristic of the LS complex [64]. At 323 K, the peak at 1416 cm^{-1} disappeared and was replaced by a new peak at 1401 cm^{-1}, a typically observed change in IR spectra during the spin crossover of iron(II) 1,2,4-triazole complexes. When the dispersion was cooled to 293 K, the wavenumber of the ν(C=N) band did not change, but further cooling to 278 K shifted it back to 1413 cm^{-1}. The hysteretic change of ν(C=N) band is consistent with those observed in SQUID and UV-vis measurements. On the other hand, the C=O stretching (ν(C=O)) and N-H vending (δ(N-H)) peaks from the amido group were maintained in the temperature range from 278 K to 323 K. This indicates that hydrogen bonds are maintained during the process of spin crossover between LS and HS species in this temperature range, which contributes to stabilizing the coordination polymer structure in chloroform solution. It is also likely that the appearance of hysteresis is due to the recombination of hydrogen bonds during the cooling process.

$[Fe^{II}(\mathbf{2})_3]Cl_2$ and $[Fe^{II}(\mathbf{3})_3]Cl_2$ showed the different temperature-dependence in FT-IR spectra (Figure S3b,c). In the case of $[Fe^{II}(\mathbf{4})_3]Cl_2$ and $[Fe^{II}(\mathbf{5})_3]Cl_2$, not only a gradual change of ν(C=N) band but also the red shift of ν(C=O) on heating was observed ($[Fe^{II}(\mathbf{4})_3]Cl_2$, 1643 cm^{-1} at 278 K, 1651 cm^{-1} at 323 K, Figure S3d,; $[Fe^{II}(\mathbf{5})_3]Cl_2$, 1649 cm^{-1} at 278 K, 1655 cm^{-1} at 323 K, Figure S3e). The reversible shift of ν(C=O) indicates that these intermolecular hydrogen bondings are formed and are not maintained at higher temperatures. Since the shorter spacer methylene length between the alkoxy chain and the triazole ring in $[Fe^{II}(\mathbf{1})_3]Cl_2$ led to the maintenance of hydrogen bonding, whether hydrogen bonding works strongly or not depends on the spacer chain length directly connected to the triazole complex. In amide bonds close to the triazole group, effective hydrogen bonds are formed because of the proximity of the amide groups. Still, as the spacer chain length increases, the distance between the alkyl chains extending radially from the triazole complex increases, and at high temperatures, the intermolecular hydrogen bonds become easily broken due to the increased thermal fluctuations of the alkyl chains. Consequently, in $[Fe^{II}(\mathbf{4})_3]Cl_2$ and $[Fe^{II}(\mathbf{5})_3]Cl_2$, the radially extended alkyl chains become less susceptible to hydrogen bonding, which weakens the intermolecular interactions necessary for jelly-like formation. As a result, these complexes are presumed to be dispersed as solutions rather than forming jelly-like states.

After the dispersions of iron triazole complexes in chloroform were freeze-dried, wide-angle X-ray diffraction was measured for dried powder of $[Fe^{II}(\mathbf{1})_3]Cl_2$ at 223 K and 373 K (Figure 5). $[Fe^{II}(\mathbf{1})_3]Cl_2$ showed the 001, 002, and 003 Bragg peaks, respectively. These diffraction peaks indicate the presence of a lamellar structure with a long period of 41.0 Å. The heating of the powder samples of $[Fe^{II}(\mathbf{1})_3]Cl_2$ increases a lamellar d-spacing to 44.5 Å. The increase in the long spacing is consistent with the melting of long alkyl chains and the changes in the molecular orientation of lipophilic alkyl chains [47,49,51,52]. $[Fe^{II}(\mathbf{L''})_3]Cl_2$ (**L''** = **3**–**5**) also produced a lamellar structure with the increase of d-spacing depending on temperature (Figure S4b–d). It indicates the introduction of the alkyl chains with ether-linkage effectively decouples the alignment of alkyl chains from the radially oriented chains around the iron triazole complex. Previous reports on 4-alkylated triazole complexes form anisotropic, rodlike structures with organic substituents radially attached to the main chains [13,23,33,34,64–68]. In the present system, introducing the ether linkage into the alkyl chain moiety has effectively decoupled the alignment of alkyl chains from linear Fe^{II} tris-triazole main chains, thereby allowing the formation of regular lamellar structures. In addition, it also seems to separate van der Waals interaction among alkyl chains from hydrogen bonding of amido-linkage. In contrast, the complex $[Fe^{II}(\mathbf{2})_3]Cl_2$ exhibited a decrease in d-spacing upon heating (see Figure S4a), suggesting that it adopts a distinct molecular packing mode compared to its analogues with other spacer lengths. This distinctive structural behavior aligns with the spin crossover properties observed in UV-vis spectroscopy, where $[Fe^{II}(\mathbf{2})_3]Cl_2$ did not exhibit a thermal hysteresis profile that diverged from those observed in complexes with longer or shorter spacers. Furthermore, FT-IR analysis revealed that the C=O stretching vibration for $[Fe^{II}(\mathbf{2})_3]Cl_2$ appears at 1651 cm^{-1} (Figure S3b), which is at lower energy compared to $[Fe^{II}(\mathbf{1})_3]Cl_2$ and $[Fe^{II}(\mathbf{3})_3]Cl_2$, and shows negligible thermal dependence. These results suggest that the hydrogen bonding mode in $[Fe^{II}(\mathbf{2})_3]Cl_2$ is less susceptible to thermal fluctuations, indicating the presence of a relatively weak hydrogen-

bonding environment. Given that the distance from the triazole ring to the amide group in $[Fe^{II}(\mathbf{2})_3]Cl_2$ is neither excessively short nor long, it is likely that ether intramolecular hydrogen bonding involving intermolecular hydrogen bonding between the alkyl chains moderately contributes to the observed spin crossover behavior and molecular packing characteristics. These findings highlight the crucial role of spacer length in regulating hydrogen-bonding interactions and spin-state dynamics in lipophilic iron(II) triazole complexes.

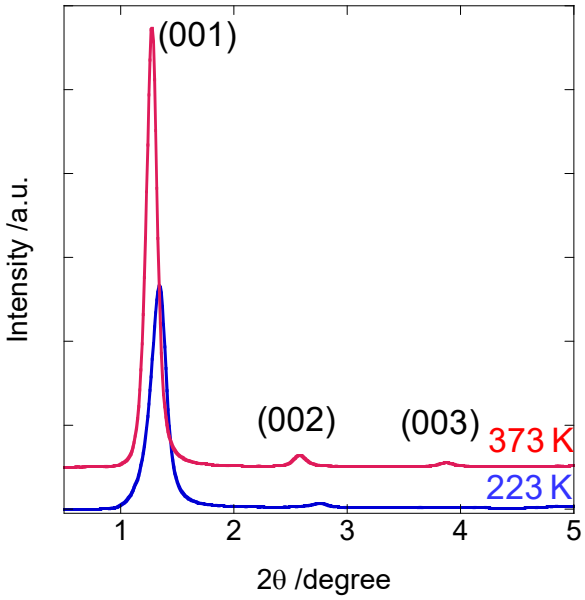

Figure 5. WAXS profiles of freeze-dried samples from $[Fe(\mathbf{1})_3]Cl_2$ in chloroform (5 unit mM) at 223 K and 373 K.

4. Conclusions

In conclusion, we have investigated the spin crossover phenomena of lipophilic iron triazole complex in organic media. Regarding nanofibrous dispersions in organic media, this is the first example of spin crossover with thermal hysteresis. A few works have been reported as lipophilic iron triazole complex in organic media to date. However, there has been no example of spin crossover with thermal hysteresis since the 3D interaction among triazole chain chains is weak in organic media [46,48,49,51,54]. It is to be noted that hydrogen bonding plays a key role in realizing spin crossover phenomena with hysteresis. The spacer length between the alkoxy chain and triazole ring is essential to the effective formation of hydrogen bonding from amide bondings, which is critical in determining the spin crossover characteristics. Introducing lipophilic chain units around coordination polymers is essential to convert solid-state pseudo-one dimensional complexes to flexible, soluble supramolecular nanowires. The effective use of hydrogen bonding contributes to stabilizing the coordination polymers in solution and creates bistable properties in thermally induced dynamic structural changes. These findings will be widely used to create functional, soft, and innovative functional coordination polymers.

Supplementary Materials: Synthetic procedures, Thermal dependence of UV-vis spectra, TEM images, FT-IR spectra, and WAXD pattern can be downloaded at https://media.sciltp.com/articles/others/2506051646541837/MI-777-SI.pdf.

Author Contributions: K.K., N.K.: conceptualization, methodology, writing—original draft preparation, reviewing and editing, TEM imaging, visualization, investigation; Y.J.: data collection, visualization, software; All authors have read and agreed to the published version of the manuscript.

Funding: This work is supported by a Grant-in-Aid for Scientific Research (A) (No. 19205030) from the Japan Society for the Promotion of Science and by JST CREST.

Data Availability Statement: Raw data will be made available upon reasonable request.

Acknowledgments: This work was supported by a Grant-in-Aid for Scientific Research (A) (No. 19205030) from the Japan Society for the Promotion of Science and by JST CREST. We also thank the Japan Synchrotron Radiation Research Institute as part of the Nanotechnology Support Project of the Ministry of Education, Culture, Sports, Science and Technology, for the approval of the synchrotron radiation experiments at SPring-8 (Hyogo, Japan).

Conflicts of Interest: The authors declare no conflict of interest.

References

1. Gütlich, P.; Goodwin, H.A. *Spin Crossover in Transition Metal Compounds I*; Springer: Berlin/Heidelberg, Germany, 2004.
2. Kahn, O.; Kröber, J.; Jay, C. Spin Transition Molecular Materials for displays and data recording. *Adv. Mater.* **1992**, *4*, 718–728.
3. Kahn, O.; Martinez, C.J. Spin-Transition Polymers: From Molecular Materials Toward Memory Devices. *Science* **1998**, *279*, 44–48.
4. Weber, B.; Kaps, E.; Weigand, J.; Carbonera, C.; Letard, J.F.; Achterhold, K.; Parak, F.G. Cooperative Iron(II) spin crossover complexes with N_4O_2 coordination sphere. *Inorg. Chem.* **2008**, *47*, 487–496.
5. Bronisz, R. 1,4-Di(1,2,3-triazol-1-yl)butane as building block for the preparation of the iron(II) spin-crossover 2D coordination polymer. *Inorg. Chem.* **2005**, *44*, 4463–4465.
6. Niel, V.; Martinez-Agudo, J.M.; Munoz, M.C.; Gaspar, A.B.; Real, J.A. Cooperative spin crossover behavior in cyanide-bridged Fe(II)-M(II) bimetallic 3D Hofmann-like networks (M = Ni, Pd, and Pt). *Inorg. Chem.* **2001**, *40*, 3838–3839.
7. Real, J.A.; Gaspar, A.B.; Niel, V.; Muñoz, M.C. Communication between iron(II) building blocks in cooperative spin transition phenomena. *Coord. Chem. Rev.* **2003**, *236*, 121–141.
8. Galet, A.; Munoz, M.C.; Gaspar, A.B.; Real, J.A. Architectural isomerism in the three-dimensional polymeric spin crossover system $[Fe(pmd)_2[Ag(CN)_2]_2]$: Synthesis, structure, magnetic properties, and calorimetric studies. *Inorg. Chem.* **2005**, *44*, 8749–8755.
9. Munoz, M.C.; Gaspar, A.B.; Galet, A.; Real, J.A. Spin-crossover behavior in cyanide-bridged iron(II)-silver(I) bimetallic 2D Hofmann-like metal-organic frameworks. *Inorg. Chem.* **2007**, *46*, 8182–8192.
10. Agusti, G.; Gaspar, A.B.; Munoz, M.C.; Real, J.A. Thermal- and pressure-induced cooperative spin transition in the 2D and 3D coordination polymers $Fe(5\text{-}Br\text{-}pmd)_z[M(CN)_x]_y$ ($M=Ag^{I}$, Au^{I}, Ni^{II}, Pd^{II}, Pt^{II}). *Inorg. Chem.* **2007**, *46*, 9646–9654.
11. Agusti, G.; Munoz, M.C.; Gaspar, A.B.; Real, J.A. Spin-crossover behavior in cyanide-bridged iron(II)-gold(I) bimetallic 2D Hofmann-like metal-organic frameworks. *Inorg. Chem.* **2008**, *47*, 2552–2561.
12. Bonhommeau, S.; Molnar, G.; Galet, A.; Zwick, A.; Real, J.A.; McGarvey, J.J.; Bousseksou, A. One shot laser pulse induced reversible spin transition in the spin-crossover complex $[Fe(C_4H_4N_2)Pt(CN)_4]$ at room temperature. *Angew. Chem. Int. Ed. Engl.* **2005**, *44*, 4069–4073.
13. Krober, J.; Codjovi, E.; Kahn, O.; Groliere, F.; Jay, C. A spin transition system with a thermal hysteresis at room temperature. *J. Am. Chem. Soc.* **1993**, *115*, 9810–9811.
14. Nakamoto, A.; Ono, Y.; Kojima, N.; Matsumura, D.; Yokoyama, T.; Liu, X.J.; Moritomo, Y. Spin transition and its photo-induced effect in spin crossover complex film based on $[Fe(II)(trz)_3]$. *Synth. Met.* **2003**, *137*, 1219–1220.
15. Nakamoto, A.; Ono, Y.; Kojima, N.; Matsumura, D.; Yokoyama, T. Spin Crossover Complex Film, $[Fe^{II}(H\text{-}trz)_3]$-Nafion, with a Spin Transition around Room Temperature. *Chem. Lett.* **2003**, *32*, 336–337.
16. Nakamoto, A.; Kojima, N.; XiaoJun, L.; Moritomo, Y.; Nakamura, A. Demonstration of the thermally induced high spin–low spin transition for a transparent spin crossover complex film $[Fe(II)(H\text{-}trz)_3]$-Nafion (trz = triazole). *Polyhedron* **2005**, *24*, 2909–2912.
17. Lee, S.W.; Lee, J.W.; Jeong, S.H.; Park, I.W.; Kim, Y.M.; Jin, J.I. Processable magnetic plastics composites—Spin crossover of PMMA/Fe(II)-complexes composites. *Synth. Met.* **2004**, *142*, 243–249.
18. Schwarzenbacher, G.; Gangl, M.S.; Goriup, M.; Winter, M.; Grunert, M.; Renz, F.; Linert, W.; Saf, R. Preparation and Radical Oligomerization of an Fe(II) Complex without Loss of Spin-Crossover Properties. *Monatsh. Chem.* **2001**, *132*, 519–529.
19. Saf, R.; Schwarzenbacher, G.; Mirtl, C.; Hayn, G.; Hobisch, J.; Gatterer, K. Synthesis of Poly(ethylene oxide)s with 1,2,4-Triazol-4-yl End Groups—Macroligands for Bistable Metal—Polymer Complexes. *Macromol. Rapid Commun.* **2004**, *25*, 911–915.
20. Enriquez-Cabrera, A.; Rapakousiou, A.; Piedrahita Bello, M.; Molnár, G.; Salmon, L.; Bousseksou, A. Spin crossover polymer composites, polymers and related soft materials. *Coord. Chem. Rev.* **2020**, *419*, 213396.
21. Coronado, E.; Galán-Mascarós, J.R.; Monrabal-Capilla, M.; García-Martínez, J.; Pardo-Ibáñez, P. Bistable Spin-Crossover Nanoparticles Showing Magnetic Thermal Hysteresis near Room Temperature. *Adv. Mater.* **2007**, *19*, 1359–1361.
22. Gural'skiy, I.A.; Quintero, C.M.; Molnar, G.; Fritsky, I.O.; Salmon, L.; Bousseksou, A. Synthesis of spin-crossover nano- and micro-objects in homogeneous media. *Chem. Eur. J.* **2012**, *18*, 9946–9954.
23. Gaspar, A.B.; Ksenofontov, V.; Seredyuk, M.; Gütlich, P. Multifunctionality in spin crossover materials. *Coord. Chem. Rev.* **2005**, *249*, 2661–2676.
24. Roubeau, O. Triazole-based one-dimensional spin-crossover coordination polymers. *Chem. Eur. J.* **2012**, *18*, 15230–15244.
25. Gaspar, A.B.; Seredyuk, M. Spin crossover in soft matter. *Coord. Chem. Rev.* **2014**, *268*, 41–58.
26. Koudriavtsev, A.B.; Linert, W. Thermally Induced Spin Crossover in the Liquid State: The Effects of Non-Ideality. *Monatsh. Chem.* **2001**, *132*, 235–243.

27. Toftlund, H. Spin Equilibrium in Solutions. *Monatsh. Chem.* **2001**, *132*, 1269–1277.
28. Turner, J.W.; Schultz, F.A. Intramolecular and Environmental Contributions to Electrode Half-Reaction Entropies of $M(tacn)_2^{3+/2+}$ (M = Fe, Co, Ni, Ru; tacn = 1,4,7-Triazacyclononane) Redox Couples. *Inorg. Chem.* **1998**, *38*, 358–364.
29. Turner, J.W.; Schultz, F.A. Solution characterization of the iron(II) bis(1,4,7-triazacyclononane) spin-equilibrium reaction. *Inorg. Chem.* **2001**, *40*, 5296–5298.
30. Schenker, S.; Stein, P.C.; Wolny, J.A.; Brady, C.; McGarvey, J.J.; Toftlund, H.; Hauser, A. Biphasic behavior of the high-spin-->low-spin relaxation of $[Fe(btpa)](PF_6)_2$ in solution (btpa = *N*,*N*,*N'*,*N'*-tetrakis(2-pyridylmethyl)-6,6′-bis(aminomethyl)-2,2′- bipyridine). *Inorg. Chem.* **2001**, *40*, 134–139.
31. Tsubasa, A.; Otsuka, S.; Maekawa, T.; Takano, R.; Sakurai, S.; Deming, T.J.; Kuroiwa, K. Development of hybrid diblock copolypeptide amphiphile/magnetic metal complexes and their spin crossover with lower-critical-solution-temperature(LCST)-type transition. *Polymer* **2017**, *128*, 347–355.
32. Fujitsuka, M.; Araki, K.; Kodama, T.; Hien, T.T.D.; Sakuragi, M.; Shetty, S.S.; Koyama, Y.; Kuroiwa, K. Supramolecular Control of Spin Equilibrium and Oxidation State in Nanohybrids of Amphiphilic Glycyrrhetinic Acid Derivatives with $[Fe(TACN)_2]^{2+}$. *Chem. Lett.* **2021**, *50*, 1142–1145.
33. Roubeau, O.; Colin, A.; Schmitt, V.; Clerac, R. Thermoreversible gels as magneto-optical switches. *Angew. Chem. Int. Ed. Engl.* **2004**, *43*, 3283–3286.
34. Fujigaya, T.; Jiang, D.L.; Aida, T. Spin-crossover physical gels: A quick thermoreversible response assisted by dynamic self-organization. *Chem. Asian J.* **2007**, *2*, 106–113.
35. Grondin, P.; Roubeau, O.; Castro, M.; Saadaoui, H.; Colin, A.; Clerac, R. Multifunctional gels from polymeric spin-crossover metallo-gelators. *Langmuir* **2010**, *26*, 5184–5195.
36. Echeverría, C.; Rubio, M.; Mitchell, G.R.; López, D. Structure of a spin-crossover Fe(II)-1,2,4-triazole polymer complex gel in toluene. Small angle neutron scattering and viscoelastic studies. *Eur. Polym. J.* **2014**, *53*, 238–245.
37. Sánchez-Ferrer, A.; Bräunlich, I.; Ruokolainen, J.; Bauer, M.; Schepper, R.; Smith, P.; Caseri, W.; Mezzenga, R. Gels, xerogels and films of polynuclear iron(ii)–aminotriazole spin-crossover polymeric complexes. *RSC Adv.* **2014**, *4*, 60842–60852.
38. Gural'skiy, I.A.; Reshetnikov, V.A.; Szebesczyk, A.; Gumienna-Kontecka, E.; Marynin, A.I.; Shylin, S.I.; Ksenofontov, V.; Fritsky, I.O. Chiral spin crossover nanoparticles and gels with switchable circular dichroism. *J. Mater. Chem. C* **2015**, *3*, 4737–4741.
39. Luo, Y.-H.; Dong, H.; Ma, S.-H.; Zeng, F.-L.; Jin, X.-T.; Liu, M. Atmospheric humidity-triggered reversible spin-state switching. *J. Mater. Chem. A* **2023**, *11*, 1232–1238.
40. Luo, Y.H.; Jin, X.T.; Zhang, S.X.; Xue, C.; Liu, M. Dynamic Aggregation Triggering Reversible Spin-State Switching. *ACS Appl. Mater. Interfaces* **2023**, *15*, 48365–48374.
41. Zeng, F.L.; Jin, X.T.; Zhao, J.; Zhang, S.X.; Xue, C.; Luo, Y.H. Construction and screening of spin-crossover-sponge materials based on iron(II)-triazole coordination polymers. *Dalton Trans.* **2024**, *53*, 2333–2340.
42. Luo, Y.-H.; Xue, C.; Zhang, S.-X.; Zhao, J.; Jin, X.-T.; Liu, M. Charge transfer-triggered reversible spin-state switching. *J. Mater. Chem. C* **2024**, *12*, 1693–1700.
43. Real, J.A.; Gaspar, A.B.; Munoz, M.C. Thermal, pressure and light switchable spin-crossover materials. *Dalton Trans.* **2005**, *12*, 2062–2079.
44. Ortega-Villar, N.; Thompson, A.L.; Munoz, M.C.; Ugalde-Saldivar, V.M.; Goeta, A.E.; Moreno-Esparza, R.; Real, J.A. Solid- and solution-state studies of the novel mu-dicyanamide-bridged dinuclear spin-crossover system $[(Fe(bztpen)]_2[\mu\text{-}N(CN)_2](PF_6)_3\cdot nH_2O$. *Chem. Eur. J.* **2005**, *11*, 5721–5734.
45. Bryliakov, K.P.; Duban, E.A.; Talsi, E.P. The Nature of the Spin-State Variation of $[Fe^{II}(BPMEN)(CH_3CN)_2](ClO_4)_2$ in Solution. *Eur. J. Inorg. Chem.* **2004**, *2005*, 72–76.
46. Kimizuka, N.; Shibata, T. Linear transition metal complexes of lipophilic triazoles and their thermochromism in cast films. *Polym. Prepr. Jpn.* **2000**, *49*, 3774.
47. Kuroiwa, K.; Shibata, T.; Takada, A.; Nemoto, N.; Kimizuka, N. Heat-set gel-like networks of lipophilic Co(II) triazole complexes in organic media and their thermochromic structural transitions. *J. Am. Chem. Soc.* **2004**, *126*, 2016–2021.
48. Kuroiwa, K.; Shibata, T.; Sasaki, S.; Ohba, M.; Takahara, A.; Kunitake, T.; Kimizuka, N. Supramolecular control of spin-crossover phenomena in lipophilic Fe(II)-1,2,4-triazole complexes. *J. Polym. Sci. Part A Polym. Chem.* **2006**, *44*, 5192–5202.
49. Kume, S.; Kuroiwa, K.; Kimizuka, N. Photoresponsive molecular wires of Fe^{II} triazole complexes in organic media and light-induced morphological transformations. *Chem. Commun.* **2006**, *23*, 2442–2444.
50. Kuroiwa, K.; Kimizuka, N. Coordination Structure Changes of Linear Cobalt(II) Triazole Complexes Induced by Binding of Long-chained Alcohols: Adaptive Molecular Clefts. *Chem. Lett.* **2008**, *37*, 192–193.
51. Matsukizono, H.; Kuroiwa, K.; Kimizuka, N. Self-assembly-directed Spin Conversion of Iron(II) 1,2,4-Triazole Complexes in Solution and Their Effect on Photorelaxation Processes of Fluorescent Counter Ions. *Chem. Lett.* **2008**, *37*, 446–447.

52. Kuroiwa, K.; Kikuchi, H.; Kimizuka, N. Spin crossover characteristics of nanofibrous Fe(II)-1,2,4-triazole complexes in liquid crystals. *Chem. Commun.* **2010**, *46*, 1229–1231.
53. Kuroiwa, K.; Kimizuka, N. Self-assembly and functionalization of lipophilic metal-triazole complexes in various media. *Polym. J.* **2012**, *45*, 384–390.
54. Matsukizono, H.; Kuroiwa, K.; Kimizuka, N. Lipid-packaged linear iron(II) triazole complexes in solution: Controlled spin conversion via solvophobic self-assembly. *J. Am. Chem. Soc.* **2008**, *130*, 5622–5623.
55. Vos, G.; De Graaff, R.A.G.; Haasnoot, J.G.; Van der Kraan, A.M.; De Vaal, P.; Reedijk, J. Crystal structure at 300 and 105 K, magnetic properties and Moessbauer spectra of bis(triaquatris(4-ethyltriazole-N^1)iron(II)-N^2,$N^{2'}$,$N^{2''}$)iron(II) hexakis(trifluoromethanesulfonate). A linear, trinuclear iron(II) compound, showing a unique high-spin-low-spin transition of the central iron atom. *Inorg. Chem.* **1984**, *23*, 2905–2910.
56. Kimizuka, N.; Shimizu, M.; Fujikawa, S.; Fujimura, K.; Sano, M.; Kunitake, T. AFM Observation of Organogel Nanostructures on Graphite in the Gel-Assisted Transfer Technique. *Chem. Lett.* **1998**, *27*, 967–968.
57. Kimizuka, N.; Kawasaki, T.; Kunitake, T. Self-organization of bilayer membranes from amphiphilic networks of complementary hydrogen bonds. *J. Am. Chem. Soc.* **1993**, *115*, 4387–4388.
58. Kimizuka, N.; Kawasaki, T.; Kunitake, T. Thermal Stability and Specific Dye Binding of a Hydrogen-Bond-Mediated Bilayer Membrane. *Chem. Lett.* **1994**, *23*, 33–36.
59. Kimizuka, N.; Kawasaki, T.; Kunitake, T. Spectral Characteristics and Molecular Orientation of Azobenzene-Containing Hydrogen-Bond-Mediated Bilayer Membranes. *Chem. Lett.* **1994**, *23*, 1399–1402.
60. Kimizuka, N.; Kawasaki, T.; Hirata, K.; Kunitake, T. Tube-like Nanostructures Composed of Networks of Complementary Hydrogen Bonds. *J. Am. Chem. Soc.* **1995**, *117*, 6360–6361.
61. Kimizuka, N.; Kawasaki, T.; Hirata, K.; Kunitake, T. Supramolecular Membranes. Spontaneous Assembly of Aqueous Bilayer Membrane via Formation of Hydrogen Bonded Pairs of Melamine and Cyanuric Acid Derivatives. *J. Am. Chem. Soc.* **1998**, *120*, 4094–4104.
62. Dolenský, B.; Konvalinka, R.; Jakubek, M.; Král, V. Identification of intramolecular hydrogen bonds as the origin of malfunctioning of multitopic receptors. *J. Mol. Struct.* **2013**, *1035*, 124–128.
63. Ostaszewski, R.; Urbańczyk-Lipkowska, Z. Solution and solid-state studies on the molecular conformation of mono- and disubstituted pyridine amidoesters: The role of characteristic C-H…O and N-H…O interactions. *J. Mol. Struct.* **1999**, *474*, 197–206.
64. Armand, F.; Badoux, C.; Bonville, P.; Ruaudel-Teixier, A.; Kahn, O. Langmuir-Blodgett Films of Spin Transition Iron(II) Metalloorganic Polymers. 1. Iron(II) Complexes of Octadecyl-1,2,4-triazole. *Langmuir* **1995**, *11*, 3467–3472.
65. Roubeau, O.; Alcazar Gomez, J.M.; Balskus, E.; Kolnaar, J.J.A.; Haasnoot, J.G.; Reedijk, J. Spin-transition behaviour in chains of Fe^{II} bridged by 4-substituted 1,2,4-triazoles carrying alkyl tails. *New J. Chem.* **2001**, *25*, 144–150.
66. Kroeber, J.; Audiere, J.-P.; Claude, R.; Codjovi, E.; Kahn, O.; Haasnoot, J.G.; Groliere, F.; Jay, C.; Bousseksou, A. Spin Transitions and Thermal Hysteresis in the Molecular-Based Materials $[Fe(Htrz)_2(trz)](BF_4)$ and $[Fe(Htrz)_3](BF_4)_2 \cdot H_2O$ (Htrz = 1,2,4-4H-triazole; trz = 1,2,4-triazolato). *Chem. Mater.* **1995**, *6*, 1404–1412.
67. Fujigaya, T.; Jiang, D.L.; Aida, T. Switching of spin states triggered by a phase transition: Spin-crossover properties of self-assembled iron(II) complexes with alkyl-tethered triazole ligands. *J. Am. Chem. Soc.* **2003**, *125*, 14690–14691.
68. Fujigaya, T.; Jiang, D.L.; Aida, T. Spin-crossover dendrimers: Generation number-dependent cooperativity for thermal spin transition. *J. Am. Chem. Soc.* **2005**, *127*, 5484–5489.